HEAD CONTOUR EXTRACTION FROM FETAL ULTRASOUND IMAGES BY DIFFERENCE OF GAUSSIANS REVOLVED ALONG ELLIPTICAL PATHS

Alessandro Foi, Matteo Maggioni, Antonietta Pepe, Jussi Tohka

Department of Signal Processing, Tampere University of Technology
P.O. Box 553 33101 Finland antonietta.pepe@tut.fi

ABSTRACT

Our fully automatic method to compute the biparietal diameter (BPD) and occipitofrontal diameter (OFD) from fetal ultrasound images is based on fitting an ellipse modelling the head contour of the fetus to ultrasound images. This is achieved by minimizing a cost function with respect to the parameters of the ellipse using a global multiscale multistart Nelder-Mead algorithm.

1. INTRODUCTION

We here present our method to compute the biparietal diameter (BPD) and occipitofrontal diameter (OFD) from fetal ultrasound images for the competition ”Challenge US: Biometric measurements from fetal ultrasound images” organized in conjunction with the ISBI 2012 conference in Barcelona. The method is unpublished and fully automatic. It is based on fitting an ellipse modelling the head contour of the fetus to the provided ultrasound images by minimizing a cost function with respect to the parameters of the ellipse. The main ingredient of the method is the novel cost function. For a given ellipse, we obtain a surface that models the skull of the fetus by revolving a difference of Gaussians along the elliptical path. The cost function can then be written as a product of the image and the surface integrated over the image domain. The cost function is minimized globally using a multiscale multistart Nelder-Mead algorithm.

The method was evaluated on the challenge dataset which consisted of 30×3=90 images of the head acquired from fetuses at 21, 28, and 33 weeks of gestation.

2. METHOD

Pre-processing. The set of ultrasound images used in the challenge has heterogeneous contrast and an irregularly shaped black background outside of the scanned area. These features may cause the minimization of the cost functional to miss the actual position of the skull.

The following two preprocessing operations were carried out on each image z_{orig}. First, the black background was filled by extrapolating the image inside of the scanned area. This was done by a constrained iterative low-pass filtering in discrete cosine transform (DCT) domain. At each iteration, we compute the DCT spectrum of the whole image z_{orig}, zero-out all but a tiny low-frequency portion of the spectrum, obtain a low-pass version of the image by inverting the transform, and impose back the portion of the original image inside of the scanned area. Few iterations are sufficient for reaching numerical convergence. We denote the thus obtained extrapolated image as z_{extr}. Note that z_{extr} and z_{orig} coincide within the scanned area.

The second preprocessing operation consists in a regularization of contrast and intensity of z_{extr}. Also for this, we leverage DCT-domain smoothing. A low-pass version $z_{\text{extr}}^{\text{LP}}$ of z_{extr} is computed according to the above procedure, without imposing back the portion of the original image inside of the scanned area. This low-pass image is used to provide smoothly varying local normalization of the intensities of z_{extr} by dividing z_{extr} by $z_{\text{extr}}^{\text{LP}}$. This normalized image is denoted as z (see Figure 1).

The cost function for fitting the ellipse. We parametrize ellipses $E(\mathbf{a})$ with 5 parameters: center coordinates c_1, c_2, semiaxis lengths r_1, r_2, and rotation angle in radians θ, organized into the vector $\mathbf{a} = [c_1, c_2, r_1, r_2, \theta]$. A rough simplification of the principal idea of the cost function is to fit three nested elliptical annuli to the image, the centermost representing the skull of the fetus featuring high intensity values, the inner and the outer representing the surrounding area, usually featuring relatively low intensity values. The complexity of the below definitions follows from the need to make the thickness of the skull uniform along its elliptical contour. Let $h_{(x_1,x_2,\mathbf{a})}$ be the straight radial half-line leaving from the center (c_1, c_2) and passing through the point (x_1, x_2). Over the radial half-line $h_{(x_1,x_2,\mathbf{a})}$, we measure the following two quantities: the radial distance $d(x_1, x_2, \mathbf{a})$ of (x_1, x_2) from the ellipse $E(\mathbf{a})$, and the normalized radial distance $r_0(x_1, x_2, \mathbf{a})$ between (x_1, x_2) and (c_1, c_2), i.e. the distance between the two points divided by the radius of the ellipse along $h_{(x_1,x_2,\mathbf{a})}$. Define

$$g(x_1, x_2, \mathbf{a}, s) = \frac{f_s(d(x_1, x_2, \mathbf{a})) - f_t(d(x_1, x_2, \mathbf{a}))}{r_0(x_1, x_2, \mathbf{a})}$$

This research was funded by the Academy of Finland under grants 130275 and 252547, and by Tampere Graduate School in Information Science and Engineering (TISE).

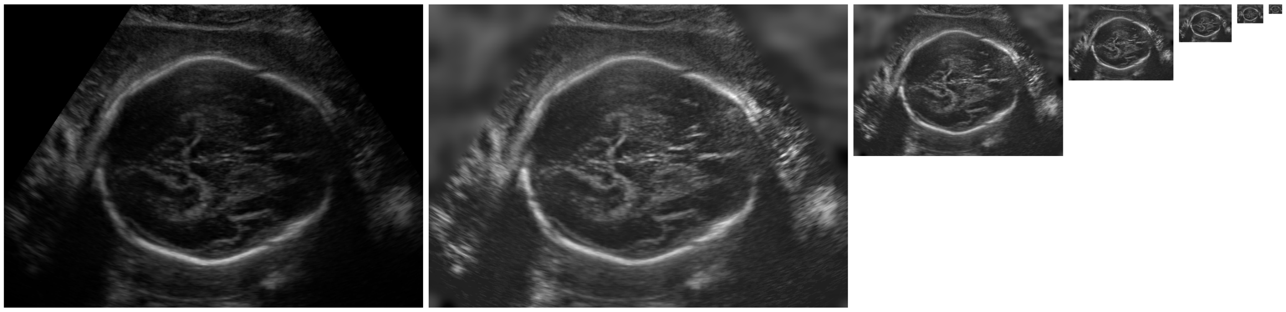

Fig. 1. From left: z_{orig}, z, and lower scale versions of z $z_{(D)}$ for $D = 2, 4, 8, 16, 32$.

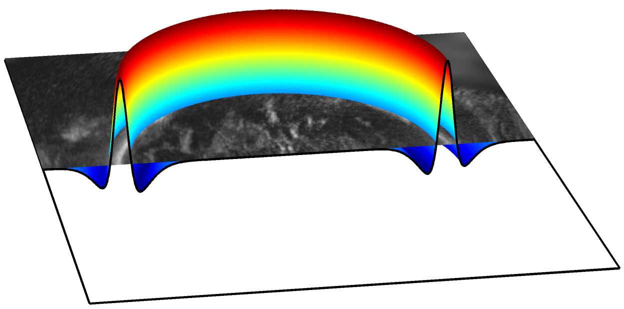

Fig. 2. Surface $g(x_1, x_2, \mathbf{a}, s)$ shown on the top of image.

where f_s and f_t are two univariate Gaussians centered at zero with standard deviations equal to s and $t = 3s$, respectively. An example of surface $g(x_1, x_2, \mathbf{a}, s)$ is shown in Figure 2. The vector $\mathbf{a}$ controls the position and shape of the ellipse fitted to the centerline of the skull, while s controls the thickness of the skull. The cost function is written as

$$\begin{aligned} C(z, \mathbf{a}, s) &= -\int\int \frac{z(x_1, x_2) g(x_1, x_2, \mathbf{a}, s)}{M(\mathbf{a})^\gamma} dx_1 dx_2 \\ &+ \lambda(\max(0, \frac{\max(r_1, r_2)}{\min(r_1, r_2)} - \text{CI}))^2, \end{aligned} \tag{1}$$

where $M(\mathbf{a})$ is the circumference of the ellipse $E(\mathbf{a})$, $\gamma = 0.6$, the regularization parameter $\lambda = 0.5$, and CI $= 1.4$ modelling the inverse of the minimal allowable cephalic index (see e.g. [1] for justification of this value). The regularization term and the exponent γ were empirically found necessary to obtain robust fits. The cost function $C(z, \mathbf{a}, s)$ is affine with respect to z and, due to the characteristics of $g(x_1, x_2, \mathbf{a}, s)$, it is not affected by the presence of large uniform regions in the image. The integral in (1) is computed as a discrete sum over the pixels.

The optimization algorithm. The cost function (1) is nonconvex with respect to $\mathbf{a}$ and s, and therefore we must use a global optimization algorithm for its minimization. In this work, we employ a multistart Nelder-Mead algorithm as follows: 1) generate a random initialization 2) run the minimization algorithm and if the minimum found is the best so far, save it; 3) apply a random perturbation to the parameters found in step 2) and go to step 2). This loop is repeated multiple times. Further, to accelerate the convergence of the optimization algorithm, we follow a coarse-to-fine approach by first fitting the ellipse on a lower-resolution version of z and then using the found fit as initialization for the ellipse-fitting on the higher-resolution image. For a given downscaling factor D, the low-resolution image $z_{(D)}$ by DCT-domain image resizing. Specifically, $z_{(D)}$ is the inverse DCT of the low-frequency portion of the spectrum of z, where this portion has the size of the desired downscaled image. Note that this is different from zeroing out the complementary portion of the spectrum (which would instead produce a full-size low-pass image). We implement this approach recursively, using dyadic downscaling factors 32, 16, 8, 4, 2, and 1 (see Figure 1). For further simplification, the standard-deviation parameter s is initially set to 0.03 times the height of the image and kept fixed while optimizing the vector $\mathbf{a}$. After convergence of $\mathbf{a}$, this optimal vector is fixed and then s is optimized.

Computation of BPD and OFD. The major and minor axes provide directly the measures of OFD and BPD, respectively, when the quantities are measured to center to center of the skull. To obtain outer-to-outer measures, we define the skull as $S = \{(x_1, x_2) : g(x_1, x_2, \mathbf{a}, s) \geq F \max(g(x_1, x_2, \mathbf{a}, s))\}$, where $F = 0.285$, compute its thickness $\Delta = \arg\max_{(x_1,x_2)\in S} \|(x_1, x_2) - (c_1, c_2)\| - \max(r_1, r_2)$. The value for F is computed based on the correction formula reported in [2]. Then, OFD and BPD are computed as $2(\max(r_1, r_2) + \Delta)$ and $2(\min(r_1, r_2) + \Delta)$, respectively. Note that we have assumed that OFD $>$ BPD, which holds for the images in the current set. The head circumference is computed with the approximate formula HC $= \pi(\text{OFD} + \text{BPD})/2$.

3. RESULTS

Evaluation. At the time of writing, we have little means for

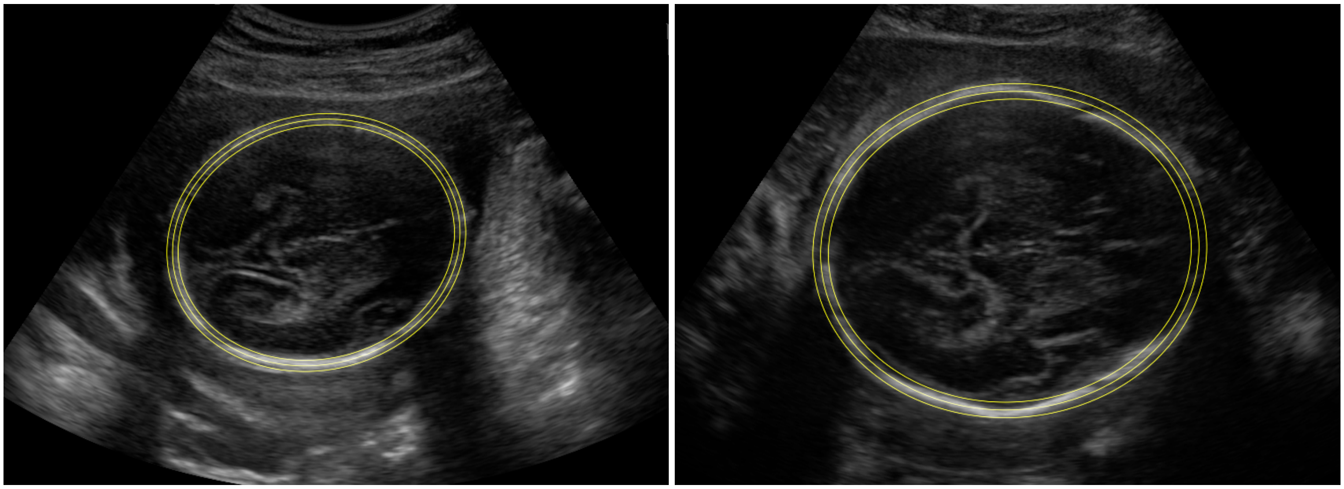

Fig. 3. Example results on 21-week old fetus (left, OFD = 64.27 mm, BDP = 54.42 mm) and 28-week old fetus (right, OFD = 89.70 mm, BDP = 76.00 mm). The central yellow contour is the fitted ellipse $E(\mathbf{a})$ and the outer yellow contour is the one used for measuring the OFD and BPD.

evaluating quantitatively the accuracy of our automatic OFD and BPD measurements, because the ground-truth measurements had not been provided to the challenge participants. However, we found that our measurements were in overall good agreement with the biometrical ranges reported in [3]. Further, based on our visual inspection, the extracted head contours were accurate for all 90 images in the dataset. Some representative results are shown in Figure 3, where the central yellow contour represents the fitted ellipse $E(\mathbf{a})$ and inner and outer yellow contours represent inner and outer boundaries of the skull. We noticed no qualitative difference in the quality of the extracted head contours between these examples and 88 other cases in the challenge dataset.

Computation time. Since the aim of this challenge was accuracy and not speed, we have purposely used an overabundant number of restarts (2010 times when $D = 32, 16$ and 10 times for other downscaling factors) and iterations of the Nelder-Mead optimization, so to ensure the highest robustness of the algorithm. With these settings, the computation time of the Matlab implementation of the complete algorithm for one image of size 756×546 pixel was approximately 5 minutes on a standard laptop (Intel Core 2 Duo CPU running at 2.6 GHz with 64-bit Windows 7 operating system). A significant portion of the computation time (over 3 minutes in each case) was spent on the optimization with the two coarsest levels ($D = 32, 16$) with the highest number of restarts. We have also prepared a lighter version of the algorithm where a significant reduction of the number of Nelder-Mead iterations decreased the computation time to half a minute while still obtaining visually identical extraction results. On a more theoretical level, the computation time is linearly related to the number of cost-function evaluations. The time required by a cost-function evaluation grows linearly with the image size and was approximately 0.1 seconds at the finest level ($D = 1$) with the above setup. Even though the code allows for a large degree of parallelization, the current Matlab implementation is single-threaded and the reported times are measured with the software running only on one CPU core.

4. CONCLUSION

We have presented a fully automatic method to compute the OFD and BDP measurements from fetal ultrasound images. The method is based on fitting an ellipse modelling the head contour of the fetus to the provided ultrasound images by minimizing a cost function with respect to the parameters of the ellipse. The main ingredient of the method is the novel cost function. For a given ellipse, we obtain a surface that models the skull of the fetus by revolving a difference of Gaussians along the elliptical path. The extracted head contours were, to our visual inspection, accurate for all 90 images, and resulting OFD and BDP measurements in good agreement with statistics in the literature on fetal biometry.

5. REFERENCES

[1] J. Kurmanavicius, E.M. Wright, P. Royston, J. Wisser, R. Huch, A. Huch, and R. Zimmermann, "Fetal ultrasound biometry: 1. head reference values," *Br J Obstet Gynaecol*, vol. 106, pp. 126 – 135, 1999.

[2] P.M. Doubilet and R.A. Greenes, "Improved prediction of gestational age from fetal head measurements," *Am J Roentgenol*, vol. 142, pp. 797 – 800, 1984.

[3] R.J.M. Snijders and K.H. Nicolaides, "Fetal biometry at 1440 weeks' gestation," *Ultrasound Obst Gyn*, vol. 4, no. 1, pp. 34 – 48, 1994.